LASER INTERFEROMETER GRAVITATIONAL WAVE OBSERVATORY

LIGO Laboratory / LIGO Scientific Collaboration

LIGO- T1000012-v6 *LIGO* 17th October 2013

HAM Large Triple Suspension (HLTS) Final Design Document

Norna A Robertson, Derek Bridges, Mark Barton, Jay Heefner, Janeen Romie, Calum Torrie, Jeff Kissel

Distribution of this document:
LIGO Scientific Collaboration

This is an internal working note
of the LIGO Laboratory.

California Institute of Technology
LIGO Project – MS 18-34
1200 E. California Blvd.
Pasadena, CA 91125
Phone (626) 395-2129
Fax (626) 304-9834
E-mail: info@ligo.caltech.edu

Massachusetts Institute of Technology
LIGO Project – NW22-295
185 Albany St
Cambridge, MA 02139
Phone (617) 253-4824
Fax (617) 253-7014
E-mail: info@ligo.mit.edu

LIGO Hanford Observatory
P.O. Box 1970
Richland WA 99352
Phone 509-372-8106
Fax 509-372-8137

LIGO Livingston Observatory
P.O. Box 940
Livingston, LA 70754
Phone 225-686-3100
Fax 225-686-7189

http://www.ligo.caltech.edu/

v2 -Table showing details of OSEMS, Magnets and DC Control Ranges (section 6) has been updated, Jan 30 2013

v3 another RODA added in section 8.1, v4 another RODA added in section 8.1, v5 added another RODA

Contents

1. Introduction

The purpose of this document is to describe the final design of the HAM Large Triple Suspension (HLTS). The HLTS will be used for the recycling optics PR3 and SR3 which are nominally 265 mm diameter by 100 mm thick. The current requirements for these suspensions are given in section 2. Responses to action items from the PDR are in section 3. The mechanical design is discussed in section 4. The electronics design is covered in section 5, with references to other documentation for the bulk of the information. Information on OSEMs and magnets and DC control ranges is given in section 6. Suspension thermal noise and seismic noise estimates are discussed in section 7. The final design review checklist is discussed in Section 8. Section 9 gives conclusions. Sections 10 and 11 give information on the MATLAB and Mathematica models respectively. Section 12 consists of appendices covering diagrams and nomenclature details of the parameters of a triple pendulum, further information on the Mathematica model, and information on input used to derive noise curves.

This document supersedes the preliminary design document T080187-00. That document gave information on the history of the design and requirements for this suspension. In particular it was noted in that document that the design of the recycling mirror suspension (the original name for the HLTS) was first developed between April 2002 and April 2003, but due to insufficient funding, work was stopped and a prototype was not built at that time. The basic idea was to scale up the input modecleaner design (now HSTS) to take the much larger recycling mirror (265 mm diameter). Because of the overall height limitations in a HAM chamber, a design with a middle mass the same dimensions as the mirror proved to be difficult to implement, and since we were not proposing to use a fibre suspension, we did not require a silica middle mass. Thus the design which was developed incorporated a metal mass whose shape resembled a cylinder truncated top and bottom. See figure 1. In mid-2007 the SUS team returned to the design of the so-called RM prototype, building on the original concept, and also focusing attention on making a stiff support

structure, further discussed in section 4. At the time of the preliminary design review of the HSTS and HLTS, the structure for the HLTS had been prototyped and tested, but the full suspension had not been fabricated. The prototype has now been fabricated and tested, and results from those tests are given in T1000106.

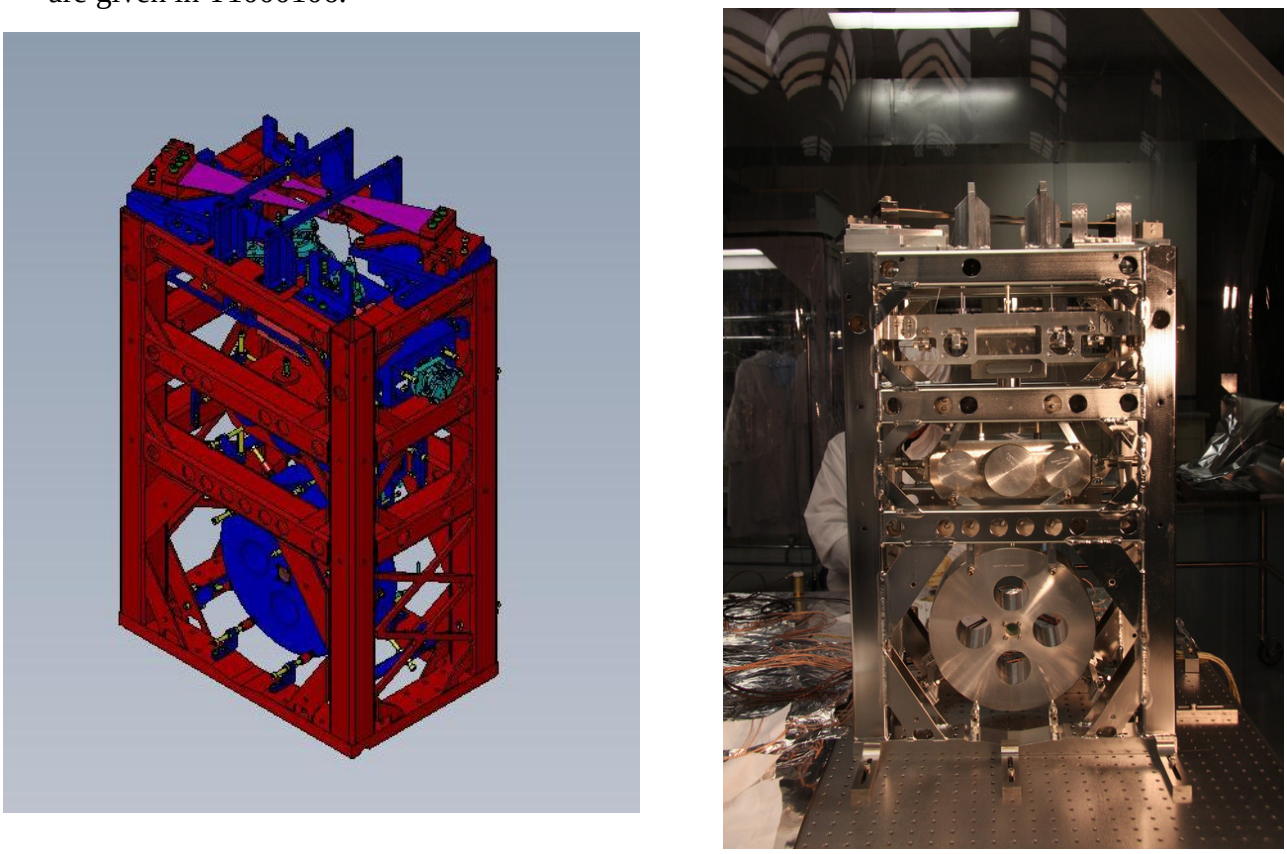

Fig 1 HAM Large Triple Suspension: left - Solidworks rendering of the final design with a dummy metal mass in place of the mirror, right – photo of the HLTS prototype assembled at LLO.

2. Requirements

The current requirements for displacement noise for the recycling cavities are laid out in the document "Displacement Noise in Advanced LIGO Triple Suspensions", M Evans and P Fritschel (T080192-01-D), and formally given in the Cavity Optic Design Requirements Document T010007-v2. The total displacement noise for the signal recycling cavity length (SCRL) is given in figure 2 of T080192. The requirement has a value at 10 Hz of 3 x 10^{-17} m/√ Hz falling to 2 x 10^{-18} m/√ Hz at 30 Hz and then flattening off. The slope from 10 to 30 Hz goes as $f^{-2.5}$. This is the *total noise* suitably summed over all the recycling cavity optics. We can make some assumptions to arrive at an approximate requirement for each optic, noting that in practice the small and large triples are similar (though not identical) in their transfer functions and suspension thermal noise estimates. From T080192, the total SRCL noise is calculated according to

$$x_{SRCL} = (x^2_{HSTS} + (2x_{HSTS})^2 + (2x_{HLTS})^2)^{1/2}. \quad \text{Eqn 1}$$

Assume that $x_{HSTS} = x_{HLTS}$. Thus the requirement for x_{HlTS} at 10 Hz is given by (3 x 10^{-17})/(√9) = 1 x 10^{-17} m/√ Hz, and at 30 Hz is given by 2 x 10^{-18}/(√9) = 6.7 x 10^{-19} m/√ Hz. As we will see later, this value is close to the expected suspension thermal noise limit for this suspension on steel wires,

making certain assumptions about the material loss and clamp design. Also the slope is the expected thermal noise slope. Thus we can meet this noise limit if residual seismic noise lies below the expected thermal noise.

We note that the requirements imposed on these suspensions are set to achieve a signal recycling cavity length noise which lies at least a factor of 10 below the aimed-for differential arm displacement noise for the interferometer, so that slightly exceeding these requirements does not immediately impact the interferometer sensitivity.

In addition to these formal requirements, there are several recommendations in T080192 which we were asked to consider. We repeat these below.

- The suspension thermal noise level is acceptable, provided the effective wire loss is close to $2x10^{-4}$, so care needs to be taken in the implementation to achieve this.
- Efforts should be made to increase the vertical seismic isolation, particularly in the 10-20 Hz band.
- Consideration should be given to making the highest vertical eigenfrequency (the `bounce mode') the same for both small and large triples (probably the higher frequency of the current small triple design is preferred).

3. Resolution of Action items from PDR

The report from the PDR is M0900018-v1. Points raised in the report and the actions taken are as follows.

3.1 Electronics

As noted on page 2 of the report, the triple electronics were not ready for review at the time of the PDR for the HSTS and HLTS. Under “Action items”, we were asked to prepare a schedule and carry out preparations for an Electronics PDR. After extensive discussions, it was agreed that the US team would took over the detailed design and prototyping of the analogue part of the triple electronics, building on the work already undertaken in the UK, to help the UK meet production schedules by accelerating the prototyping phase. This work has been carried out and subsequently reviewed at an FDR level by a team led by Vern Sandberg, and final review reports have now been issued. It has been agreed that the final design review of the US part of the electronics and the integration of the US and UK parts will take place when the HAM large triple suspension (HLTS) final design review is held, and that is what is now taking place. Further information on the electronics is given in section 5 and section 6.

3.2 28 Hz vertical peak and vertical isolation

No specific recommendations on an approach to these issues were given. We were asked to consider two paths

3.2.1 The use of higher strength maraging blades to lower vertical frequencies and hence increase isolation.

We have considered this and concluded that there is no strong advantage to using higher strength material. This is captured in RODA M0900234-v1 “SUS (US) blades will use maraging 250” The following statement appears in the RODA “Given that the creep rate of maraging 250 has been demonstrated to be low, and that only a modest increase in isolation would result from using 300, we advocate using maraging 250 in all Advanced LIGO suspensions.” Further details can be found in the RODA.

3.2.2 Determine with the SEI team if modeling indicates coupling to SEI of the 28 Hz peak and if this might present a problem.

We have been in contact with Fabrice Matichard regarding this suggestion, noting that if such coupling existed it should be seen at LASTI between the quad suspension (highest vertical mode at ~17 Hz) and the BSC-ISI, and asking if there was any evidence for this. In his reply Fabrice commented that there is nothing noticeable at 17 Hz on the BSC-ISI and in his opinion it would be more useful to spend time testing rather than modeling. Further testing may be possible when a HAM-ISI is installed at LASTI, and either an HSTS or an HLTS prototype could be put on it. Lacking any current experimental evidence that there might be a problem with the 28 Hz peak, we are not advocating any radical change to the design.

3.3 Maximum acceptable weight

We were asked to coordinate with SYS on the maximum acceptable weight for the HSTS and HLTS suspensions based on recent layout information. We are in close collaboration with SYS on this issue and will continue to liaise with them. At present the total estimated mass for the HLTS is 94.5 kg (208 lb).

4. Mechanical Design

4.1 Overall suspension design

The basic design for this suspension is based on the GEO triple pendulums (see T010103), with two key differences which are simplifications.

i) steel wires instead of silica fibres in the final stage

ii) no triple reaction pendulum for applying global control. See T020059-01-D for justification of removal of the reaction pendulum.

The key design features are as follows

- Triple pendulum with three masses of approximately equal mass and approximately equal lengths.*
- Two stages of cantilever springs made of maraging steel blades for good vertical isolation: top stage consists of two blades from which two wires go down to the top mass, and lower stage consists of four blades within the top mass with four wires going down to the intermediate mass.
- Damping of all of the low frequency modes of the triple pendulum uses 6 co-located sensors and actuators at the top mass of the triple pendulum. To achieve adequate damping the design has to be such that all the modes couple well to motion of the top mass.

- DC alignment of optic yaw and pitch is done by applying forces to the actuators at the highest mass. This requires that the intermediate mass and the optic are each suspended by four wires, two on each side, so that the system behaves like a marionette from the top mass downwards.
- Global control forces can be applied at the intermediate mass and the optic in a hierarchical manner using electromagnetic forces, with the magnets attached to the back of the masses and the coils attached to the support structure.

*The choice of equal masses and equal wire lengths as a baseline has come from experience with previous designs and leads to good coupling of modes. In addition using three equal lengths gives the best isolation for a given overall length.

The suspension has to fit within the HAM chambers. This limits the overall length of the suspension within its support structure. Currently the length from top blade to centre of optic for the large triple is approximately 0.65 m. The size of the optic (ignoring wedge) is 265 mm diameter x 100 mm thick, and mass ~ 12 kg.

The detailed set of mechanical parameters, as used in the MATLAB model with values as of March 2010, is given in Section 10. The listing includes the expected normal mode frequencies for the suspension. A set of modal shapes, derived using Mark Barton's Mathematica model of the suspension can be found at T1000136-v1. This link also contains the model files.

Diagrams and notes explaining the key nomenclature used for the triple suspension parameters are given in Section 12.

Detailed engineering drawings can be found from links on the review wiki page.

4.2 Blade design

4.2.1 Vertical isolation and stress in blades.

The blade design follows that used in GEO (which was based on the VIRGO design). The blades are approximately trapezoidal and pre-curved so that when the correct load is applied they are flattened. In the designs used for the large triple prototype being tested at LLO the blades are conservatively stressed to a level of 600 to 800 MPa, corresponding to the typical stress levels used in the GEO designs. As noted at the preliminary design review we were asked to consider making efforts to increase the vertical isolation. Using the same criteria in the triple blade designs as used for the quadruple pendulums, where a stress level up to ~1 GPa has been used, we can gain a factor of ~ 2 to 4 improvement in isolation. This is more fully discussed in T080267-00-R. We note that the HLTS prototype at LLO has blades whose design predates this shift to softer blades.

We have been prototyping blades for Advanced LIGO. Unfortunately the first round of such prototyping was not entirely successful. The company was unable to meet the specification on shape and used a procedure (a particular type of press braking) which we would not have recommended if informed beforehand. At the time of writing we have gone out to three further vendors to increase our vendor pool and allow us to check whether the highly curved blades need for the Small triple (HSTS) can be successfully produced. Preliminary results from one of the vendors suggest that such blades can be made. We have still to assess blades from the second and third vendor. When we have finished characterising all the recent blades we will be able to make a

decision about the vendor or vendors we will use for all the HAM suspensions (HSTS, OMC SUS and HLTS). Since we do not wish to hold up other procurements, we have chosen to go ahead with this FDR with the proviso that the blade procurements are not yet ready to be placed. We note however that the revised softer HLTS blades are not as challenging to make as the highly curved ones for the HSTS.

4.2.2 Nickel Plating and Production of Blades

The manufacturing specification for all maraging steel blades now includes Ni-plating to mitigate corrosion. A comprehensive process specification for manufacture of all blades for Advanced LIGO has now been produced. See E090023. It includes material requirements, shaping details, detail on the nickel plating process and details of the age hardening fixture. As noted in section 3.2 above, all SUS (US) blades will use maraging 250.

4.3 Structure Design

At the time of first designing the HLTS structure, while a requirement for the resonant frequencies had not been formally captured, it was understood that the structure should not have a resonant frequency below 150 Hz. This requirement was based on the need for the structure to not compromise the upper unity gain frequency of the HAM-ISI control, which is ~60 Hz. Extensive work was carried out on modeling the HLTS structure with a goal of achieving close to 150 Hz. The current design (see fig 2) consists of a welded steel structure with gussets and cross-bracing. The structure has been prototyped and results taken of the resonant frequencies. The key result is that the lowest resonant frequency when the structure is loaded essentially as it will be in use is 141 Hz. This is a very good result. The work is fully described in T080319.

Recently, in discussion with Systems and SEI, the emphasis has shifted from the frequency of such structures to their damping, and SUS has been directed to forego further efforts to push up this frequency. We have been asked to add provision for attachment of conceptual stiffening/damping struts or plates to the HLTS structures. This was originally captured in RODA M080374. At the time of writing Systems and the Stanford research group are carrying out research on the design of suitable struts or other damping methods for suspension structures. In addition Systems have been including conceptual struts in the layout on the HAM tables – see for example D0900465, and are working on the clamping arrangements. A recent RODA, M1000047-v1 captures all the changes needed in the structures to cover the interface of spacers, damping struts, corner clamps and dog clamps and this RODA is being acted upon.

We note that at the time of writing, details of the methods of overall alignment of optics and cavities, details of method(s) of installation of suspensions and details of the routing of electronics cabling have still to be finalised for Advanced LIGO. All of these need holes in the structures and some alignment techniques may require fiducial marks. We have provided a preliminary suite of holes to accommodate the alignment installation and cabling needs. These will be revised and extended to include the holes for damping struts/plates etc. With regard to positioning on the HAM table, we have also been asked to call out that the base of the structure should be deburred and that if possible the outer edge be rounded off.

To keep the mass of the structure within requirements, the walls of the steel legs are thin, and to attach some of the suspension parts self-clinching nuts were required. Their use in the prototype is summarised in T0900223. It should be noted that their use has only been approved for the HLTS

prototype at this time. We seek approval for their use for production parts from the Vacuum Review Board.

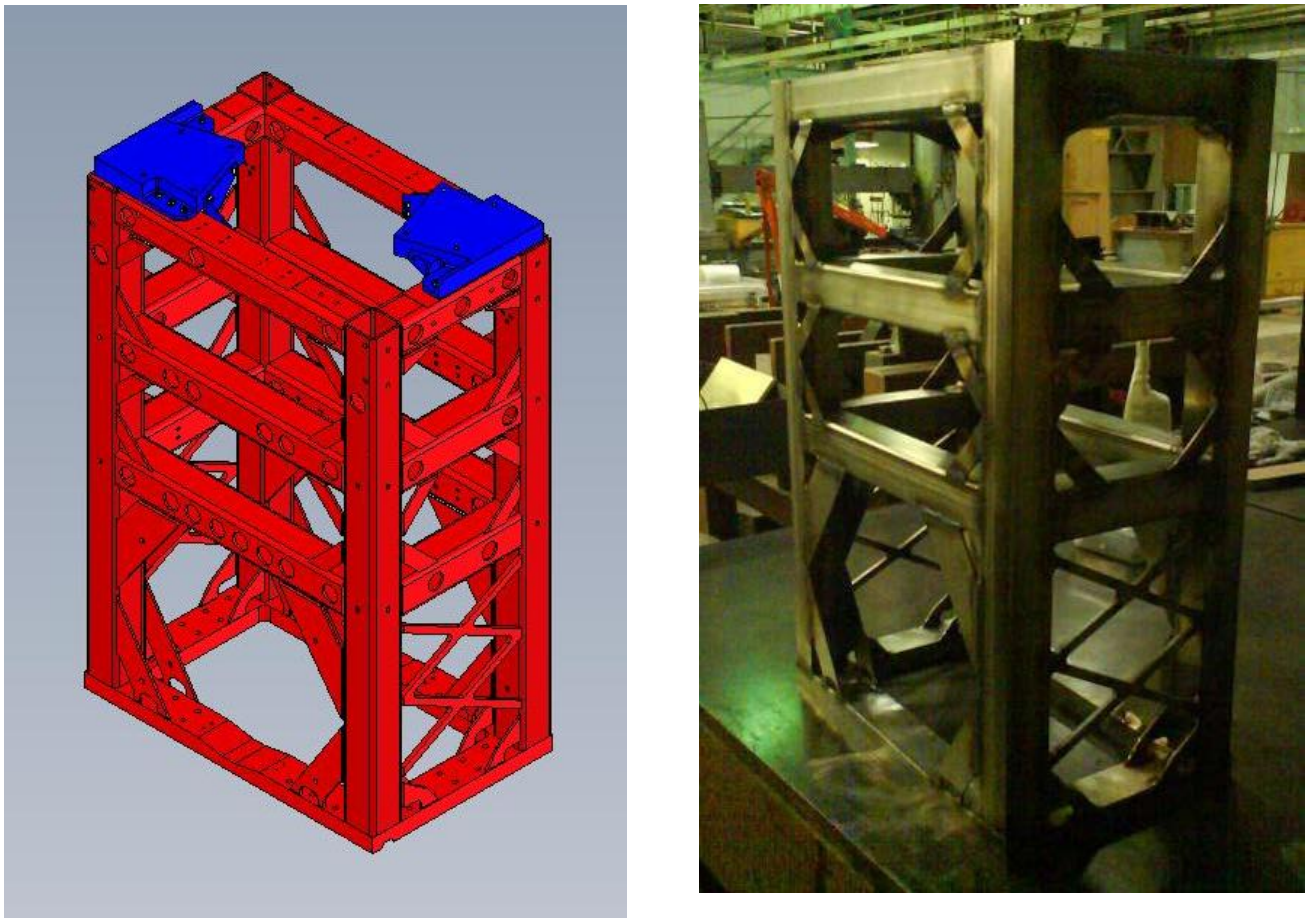

Figure 2 HLTS stainless steel support structure: left – Solidworks rendering, right – prototype set up for frequency tests

The alternative is to redesign the structure with thicker legs, possibly removing gussets and/or other changes to keep the mass approximately the same. Considerable work would be needed to produce a revised design, and hence given the tight schedule to produce these suspensions, our preference is to see if self-clinching nuts are acceptable.

4.4 Final Stage Wire Diameter

As stated in section two we were asked that consideration should be given to making the highest vertical eigenfrequency (the `bounce mode') the same for both small and large triples. The HSTS will use wire of 60 micron radius (0.12 mm diameter) giving a highest vertical mode of 27.5 Hz. In the HLTS prototype we have used 0.1345 mm radius wire, giving a predicted highest vertical mode frequency of 28.1 Hz.

4.5 Prism Design

We have adopted the double prism technique (sapphire prism with laser ablated groove and smaller steel prism below) for suspending the optic, following investigations by Rai Weiss and colleagues on losses in wire suspensions, discussed more fully in section 5 of the preliminary design document T080187. The design is more fully described in T080266-03. We have had some prototype sapphire prisms manufactured for both small and large suspensions (D0810033-v3 and D070441-v3 respectively) and the small prisms appear to satisfy our requirements. However some of the grooves in the larger ones did not appear to be to specification, being somewhat shallower than required. See figure 3. Some of the early observations of shallow grooves were due to incomplete cleaning, and a process has been developed by Bob Taylor to ensure fully clean grooves involving extended ultrasonic action in liquinox and DI water. Full inspection of all the prototype prisms is still underway, and when we have a complete picture we will communicate with our vendor to discuss the results. However we note that the UK aLIGO team have been able to procure satisfactory prisms for the upper stage of the quad suspension, so that an alternative supplier is available.

With regard to gluing these prisms in place, we have two possibilities for the sapphire prisms. We could glue them using a vacuum approved glue (replacement for vacseal) following the technique used by Rai Weiss during tests at MIT, which involves using a bead of epoxy around the perimeter of the prism but no epoxy between it and the optic. Alternatively we could use UV cure epoxy between the prism and the optic. One can use a very thin layer of this epoxy. This technique also gives less adhesive area exposed to vacuum. The lower prism can be tacked in place at each end using epoxy. The technique used by Weiss was to insert this prism between the wire and the optic while it was in the wire loop, pushing down until one feels some tension, and then tacking in

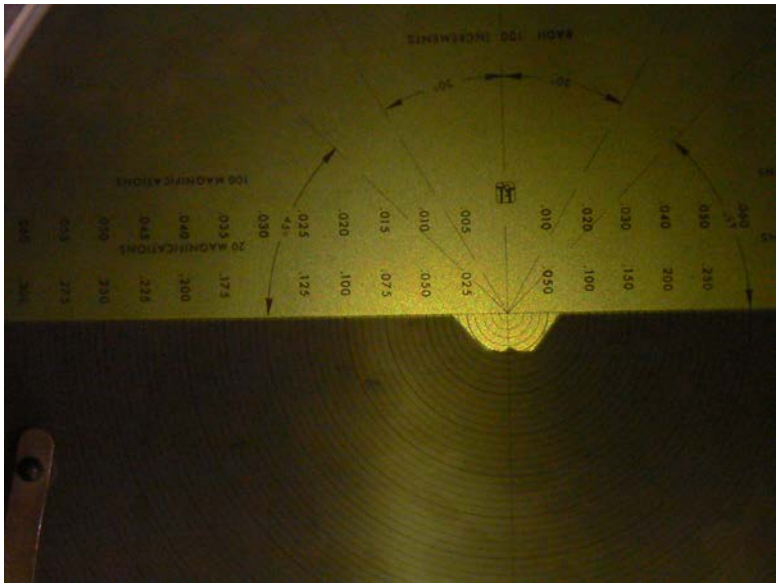

Figure 3. groove in prism showing incomplete depth.

place. However, if we wished to have ready-bonded optics prepared ahead of installation, we could determine the correct place on an actual suspension and then remove and glue the prism and store the optics till required.

4.6 Methods of Attaching Magnets

For the bottom two stages of the HLTS, the magnets with standoffs will be glued on, using an approved epoxy. The magnet/standoff assemblies are placed on each stage using a magnet placement fixture. We are using the same shadow geometry for the AOSEMs as was used in initial LIGO, and hence the magnet needs to be at the same sweet spot. The top magnets are held on magnetically to steel inserts, using the same design as used in the ETM/ITM suspensions. Renderings of the magnet/standoff arrangement for each stage are shown in Figures 4 to 6. Information on the types and sizes of magnets is given in section 6. Fixtures for placing magnets on the intermediate mass and optic are shown in figures 4 and 5. Figure 6 shows the top mass with its flags and magnets.

4.7 Methods for Adjusting Suspension for Different Masses

This suspension is used for the large recycling mirrors PR3, SR3, and F-PR3. Each of these optics has a mass (including attachments) of 12.142 kg, and a 0.6 degree asymmetric wedge oriented vertically, heavy side down (see T080078 and M080041 for wedge information). We employ several techniques for adjusting the overall mass and position of the suspension to account for variations in materials. Firstly, the upper and lower blades have a library of clamps with clamp angle increments of 0.5 degrees, ranging from 0 to ±3.5 (deg). For the upper blades, of length 25 cm, a 0.5 degree angled clamp changes the tip height by approximately 2 mm. For the lower blades, length 12 cm, a 0.5 degree angled clamp changes the tip height by approximately 1 mm. Thus angled clamps can give fairly large changes, which can be used to correct for variations of stiffness within batches of blades, noting that we will characterize all blades before use and pick matched pairs to minimize asymmetries.

Secondly, we can adjust the masses of the upper and/or intermediate masses. The upper mass has 1/4-20 bolts on the top and bottom directly in the middle of the mass to hold removable masses (see

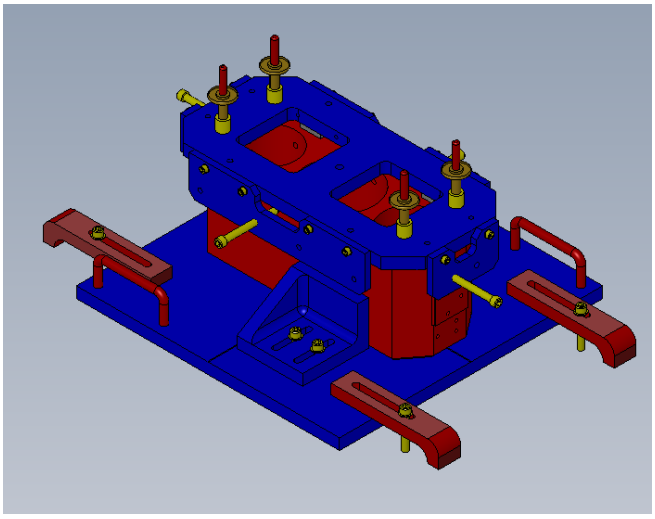

Figure 4 (left) magnet fixture jig for intermediate mass

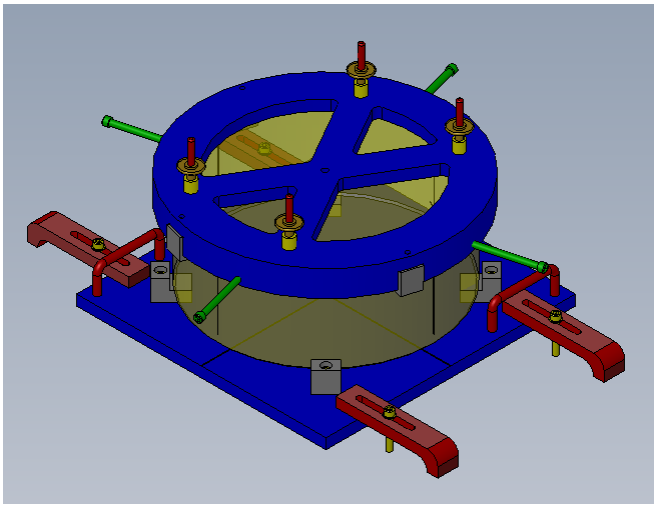

Figure 5 (right) magnet fixture jig for optic

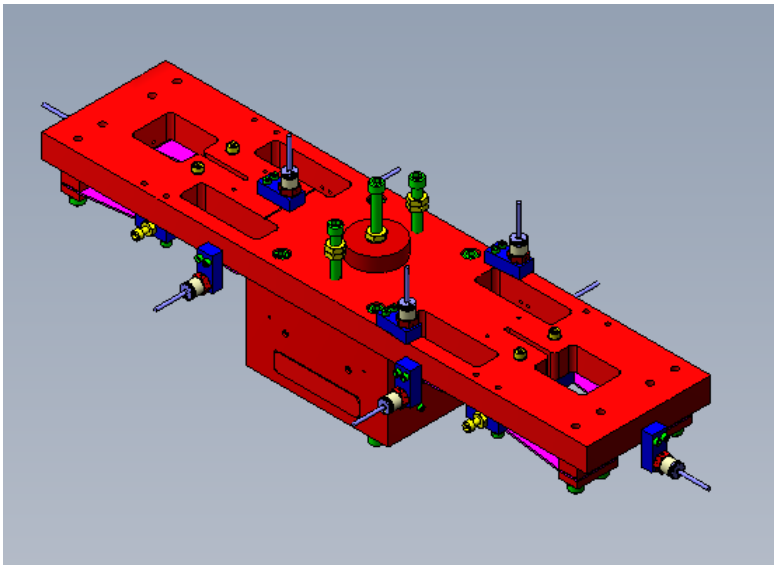

Figure 6. Top mass showing flags and magnets

D070335 Upper Mass Assembly drawing). The baseline design requires 200 grams of removable mass, so that the total mass can be adjusted upward or downward. In addition, it has provision for moving mass frontwards and backwards and left and right for trimming pitch and roll respectively. The intermediate mass has two adjustments: the first consists of two 1/4-20 bolts symmetrically offset from each side of the center of the mass so that mass can be added to both sides (right and left) evenly or, if necessary, unevenly to adjust the mass in roll (see D070334 Intermediate Mass Assembly drawing) and the second consists of a series of collars (the masses of which are 100, 300, 500, 700 and 900 grams) that fit around the center mass offset (see D080181 Intermediate Mass Changer Assembly drawing). The baseline design requires the use of the 300 gram collar and 100 grams of removable mass on the 1/4-20 bolts to allow the total mass to be adjusted upward or downward. In addition, the center mass offset and left and right mass offsets can be moved forward and back to affect the pitch of the mass. There are designs for removable masses of 50, 100 and 150 grams. The addition of 100 grams will cause a change in deflection of ~0.4 mm for the top and ~0.3 mm for the bottom blades.

4.8 Results from prototype build

These are discussed in T1000106.

5. Electronics design

Responsibility for the electronics for the HLTS is split between the UK (University of Birmingham) and the US. The UK team is making the analogue electronics for sensing and driving and the US provide the rest of the electronics and carry out the integration of all the parts. Details of the electronics for the HLTS are given in the document "aLIGO Triple Suspension Controls Design Description", J Heefner, T1000061-v1. Note that this document covers the electronics design for *all* triple suspensions (beamsplitter, folding mirror, HLTS, HSTS). Details of the usage of OSEMs in the HLTS are given in the next section.

6. OSEMs, Magnets and DC Control Ranges

The following table is captured from T1300083-v1, where more details and frequency-dependent information can be found. Any future updates to T1300083 supercede what is captured here.

HAM Large Triple Suspension (HLTS)
Details of OSEMS, Magnets, Coil Drivers and maximum DC drive range at each stage
T1300083-v1
Jeff Kissel
31st January 2013

Max DAC Voltage	(Differential voltage across the Plus and Minus legs)
[V_p]	
10	

Suspension Stage	OSEM Type	Magnet Type	Magnet Size diameter x thickness	Coil Magnet Actuation Strength	Coil Magnet Actuation Strength
Units	**[ ]**	**[ ]**	**[mm]**	**[N/A]**	**[N/mA]**
Top (TOP, M1)	BOSEM	NdFeB	10 x 10	1.694	0.001694
Intermediate Mass (MID, M2)	AOSEM	SmCo	1.905 x 3.175	0.0158	0.0000158
Optic (BOT, M3)	AOSEM	SmCo	2 x 0.5	0.00281	0.00000281

Coil Driver	DC Transconductance	DC Max Current Output	DC Current Range	DC Current Range Requirement	Frequency Range
Units	**[mA/V]**	**[mA_p]**	**[mA_pp]**	**[(mA_p) or (mA_rms)]**	**[Hz]**
Triple TOP (D0902747-v4)	11.919	119.19	238.38	60 (p), 200 (rms)	f < 1 Hz, 1 Hz < f < 100
Triple Acq. (D0901047-v4)	0.32635	3.2635	6.527	M2: 3 (p), M3: 0.15 (p)	f < 1 kHz, f < 1 kHz
Modified Triple Acq. (L1200226-v2)	2.8284	28.284	56.568	n/a	n/a

Degree of Freedom (DOF)	Stage	DC Compliance at Mass	Lever Arm	# of OSEMs	DC Compliance at Coil Driver Output	DC Max Disp. from Coil Drive	DC Max Disp. from Coil Drive	DC Disp. Range from Coil Drive	DC Disp. Range from Coil Drive
Units	**[ ]**	**[(m/N) or (rad/N.m)]**	**[m]**	**[ ]**	**[(m/mA) or (rad/mA)**	**[(m_p) or (rad_p)]**	**[(um_p) or (urad_p)]**	**[(m_pp) or (rad_pp)]**	**[(mm_pp) or (mrad_pp)]**
Longitudinal	M1	0.000547	1	2	1.852E-06	2.207E-04	220.75	4.415E-04	441.500
Pitch	M1	0.242660	0.045	2	3.700E-05	4.410E-03	4409.55	8.819E-03	8819.093
Yaw	M1	0.052898	0.08	2	1.434E-05	1.709E-03	1708.88	3.418E-03	3417.767
Longitudinal	M2	0.001360	1	4	8.593E-08	2.804E-07	0.28	5.609E-07	0.561
Pitch	M2	0.433880	0.03	4	8.226E-07	2.685E-06	2.68	5.369E-06	5.369
Yaw	M2	0.125610	0.105	4	8.335E-07	2.720E-06	2.72	5.441E-06	5.441
Longitudinal	MODM2	0.001360	1	4	8.593E-08	2.431E-06	2.43	4.861E-06	4.861
Pitch	MODM2	0.433880	0.03	4	8.226E-07	2.327E-05	23.27	4.653E-05	46.535
Yaw	MODM2	0.125610	0.105	4	8.335E-07	2.358E-05	23.58	4.715E-05	47.152
Longitudinal	M3	0.003501	1	4	3.935E-08	1.284E-07	0.13	2.569E-07	0.257
Pitch	M3	0.609230	0.104	4	7.122E-07	2.324E-06	2.32	4.648E-06	4.648
Yaw	M3	0.232780	0.06	4	1.570E-07	5.123E-07	0.51	1.025E-06	1.025

References

DAC Voltage	T1200311-v1	
OSEM and magnet details	M0900034-v4	
OSEM Coil/Magnet Actuation Strengths	T1000164-v3	
DC Compliances for long/pitch/yaw	https://redoubt.ligo-wa.caltech.edu/svn/sus/trunk/Common/MatlabTools/TripleModel_Production/	
	Model:	ssmake3MBf rev1891
	Parameters:	hltsopt_metal.m rev2034
	DC compliance ==	Transfer function from given stage drive to test mass; L to L,P to P, and Y to Y
Coil driver requirements	T080065-v1	
	Informed by	https://awiki.ligo-wa.caltech.edu/aLIGO/TripleSuspensionActuation
Coil Driver DC Transconductance	https://alog.ligo-la.caltech.edu/aLOG/index.php?callRep=4495	
Lever Arms	D070447-v2	

7. Noise Estimates

A full set of noise estimates (seismic noise, sensor noise, thermal noise, in longitudinal, vertical pitch and yaw degrees of freedom) was prepared for the preliminary design review, see T0810039. Since those graphs were produced, there have been a few changes. Firstly a bug was discovered in the thermal noise code written in Mathematica which was used to derive the thermal noise curves for wire suspensions. This is written up in T0900320. The upside is that the bug caused the thermal noise estimates to be overestimated by a factor of ~ √2 at ~10 Hz and above. Secondly there are minor changes to a few parameters using as-built numbers. The current parameter file is given in section 10.

We present in figures 7 and 8 updated noise plots for longitudinal and vertical directions. The thermal noise curves produced using Mark Barton's Mathematica model takes into account the vertical asymmetric wedge of 0.6 degrees (heavy side down). However the difference between the plots without and without a wedge is minimal. The seismic and sensor noise curves are produced using the MATLAB model T080310-v3 which assumes symmetry. The requirements are also indicated on the graphs. We again include two versions of the seismic input at the top of the suspension, as supplied by Peter Fritschel and documented in T0810039. The sensor noise curves have been produced in the same way as in T0810039 with active damping using a simple control law. The details of the seismic inputs used and the damping filter are included in sections 12.4 and 12.5 respectively. The damping was set to give decay times of approximately 10 seconds.

We note that the curves are essentially the same as presented in T0810039 except for the ~ √2 improvement in the thermal noise estimates, taking the thermal noise below the requirement except at the 28Hz vertical peak: at 10 Hz the requirement (with assumptions as presented in section 2) is 1×10^{-17} m/√ Hz, whereas the thermal noise is 9.0×10^{-18} m/√ Hz. Other conclusions are unchanged from those presented in T0810039. There is excess seismic noise in both longitudinal and vertical directions, for longitudinal up to ~ 20 Hz and for vertical up to the 28 Hz peak. We understand that steps are being taken to see if more isolation can be provided by the HAM-ISI. The sensor noise is also high in this 10-20 Hz region. As discussed in T0810039, there are several options which could be implemented to reduce that noise term including using a more aggressive control law, reducing the gain in science mode or using modal damping.

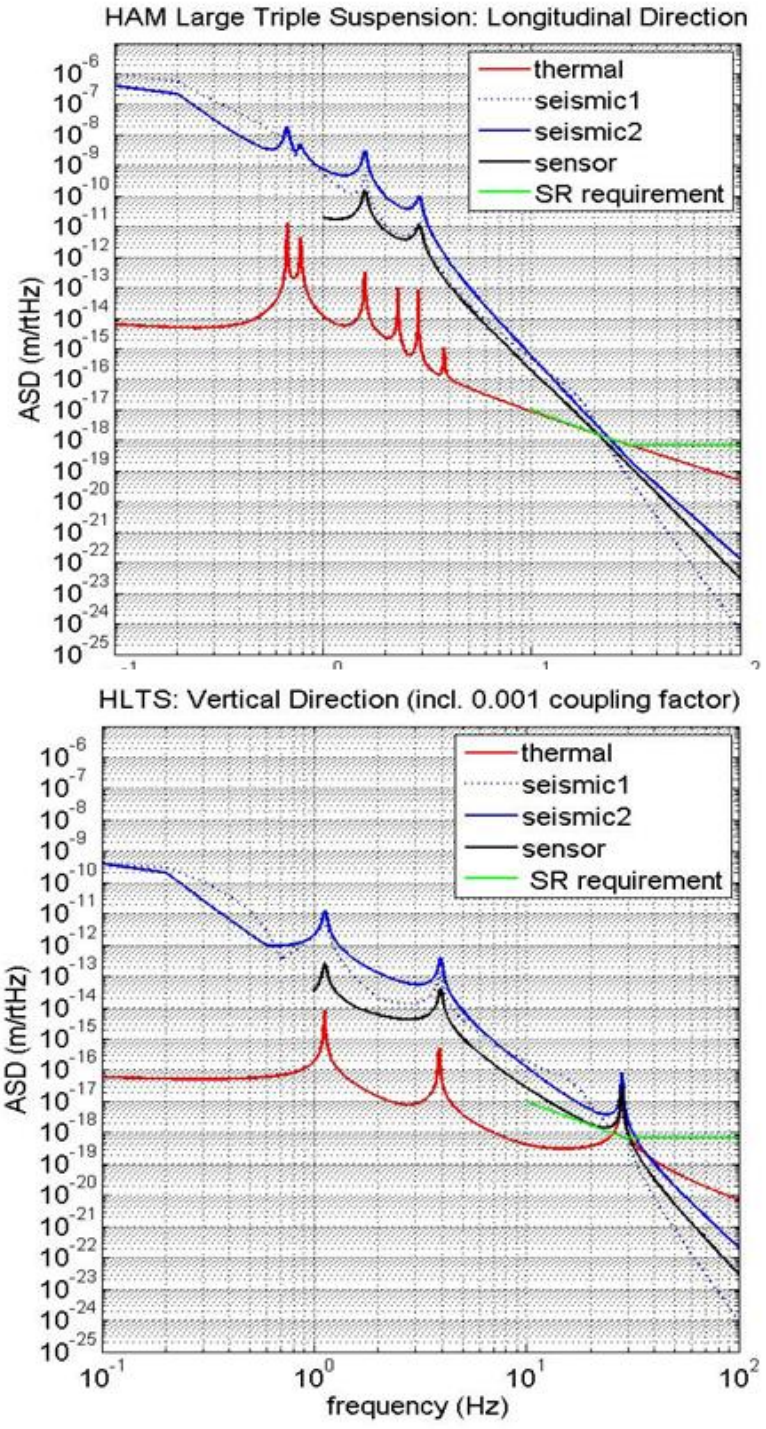

Figures 7 and 8. HLTS noise plots: longitudinal (above), vertical (below). Details as in text.

8. Final Design Review Checklist

We have taken the checklist given on page 10 of the document M050220-09, "Guidelines for Advanced LIGO Detector Construction Activities" and created an excel spreadsheet E1000053-v1. For each point on the checklist we have listed on the spreadsheet the document(s) which address that topic (where such exist). We cover below a couple of items not referred to in other documentation.

8.1 Relevant RODAs

M050397-03 "Core Optic sizes, including TMs, BS, FM and RM"

M060315-00 "No Flats on Input Mode Cleaner Optic & Recycling Mirror for Advanced LIGO"

M080038-03 "Responsibilities for Elements of the Stable Recycling Cavities"

M080041 "Thickness of PR3 and SR3 and symmetric wedge of same"

M080374-00 "HAM Triple Suspensions to have provision for mounting damping struts to the tops of their structures"

This RODA has been superceded in content by M1000047-v1 (see below).

M0900034-v3 "Magnet sizes and types and OSEM types in Adv. LIGO suspensions"

M0900087-v1 "All in vacuum cabling will be shielded"

M0900234-v1 "SUS (US) blades will use maraging 250"

M0900271-v1 "Division of Responsibilities for Harnesses for Adv. LIGO Suspensions"

M1000047-v1 "Decision to modify HAM structures (HLTS, HSTS, OMC)"

M1000312-v2 "Use of SS 316 in AOSEMs and BOSEMs".

M1100117-v2 "RODA of HSTS and HLTS stay clear area"

M1100192-v1 "RODA: Accuracy of height of mirrors in HSTS and HLTS"

All of the above RODAs have been acted on.

8.2 Relevant Risk Registry Items

RR092 "If requirements regarding front-end electronics (delivered from UK) change after delivery, then redesign and rework will be required."
The requirements have not changed from the initial requirements, but these requirements are based on models. The most probable time for changes will be during the first commissioning activities. Therefore, the risk has not changed. Hopefully we have built enough safety margin into the requirements to cover unforeseen operational modes and requirements not uncovered during the modeling phase.
RR101 "UK schedule delayed"
Mitigation actions: 1) Added US support to electronic design. 2) UK obtained award extension. Both of these have been done and we believe the triple electronics will be delivered on a schedule which meets our needs. See also RR116 below.

RR102 "Potential shortage of engineering and skilled touchlabor skills -- solidworks drafters; Conflict with S6 run operators being unavailable"
This risk has been addressed in the development phase with extra staff. We will consider extra staff in project phase if/as needed. We have also started to add staff at the sites for testing of UK and US electronics following delivery and prior to installation.

RR103 "OSEMs are complicated to make; cost or schedule overruns, difficult to find vendors"
a) AOSEMs: Mitigation taken – value engineering has been carried out. However unforeseen difficulties were encountered with first articles: 1) variable resistivity of body material – we have now identified a PEEK material with controlled characteristics which is undergoing RGA tests, 2) variable and possibly excess noise in LED/PD combination. We believe this has now been resolved, see T1000100. We can meet the requirements for sensor noise in the HAM Auxiliary suspensions as provided to us by the IO group. (The HAM Aux suspensions are the only place these OSEMS are used as *sensors*). We are working to minimise schedule delay caused by these two isseus.

b) BOSEMS: the UK group identified excess noise in LEDs as a serious problem. Current mitigations being investigated - selecting from a large population (time consuming) or changing type of LED, which will need to be UHV tested. We are working with the UK team to miminise the schedule hit which this risk is causing, and looking into a delivery schedule which will meet the revised installation plan.

RR 104 "Blade procurement: difficulty in identifying vendor, fabrication process"
This is still an open risk as described in section 4.2.

RR105 "Blade nickel plating: looking for vendor, suitable process"
Risk retired – process established and vendors identified. We note that the technical person liaising with the vendor needs to pay close attention as the work is carried out to ensure that the correct process is followed.

RR106 "Structure and welding: Vacuum, structural requirements cannot be simultaneously met".
Open mitigation actions are " Provide suitable holes in production structures for retrofitting damping struts. Investigate and evaluate effects of struts and other damping mechanisms on test structures". Holes are being provided. The investigations are ongoing by Systems, and any retrofits will be implemented as and when appropriate.

RR-107 "OSEMS: reliability, handling issues"

Mitigations- Extensive burning in of OSEMS, use in prototypes; good statistics to date. Risk retired.

RR116 "If the UK are unable to deliver all of their electronics due to their tight funding schedule, then schedule delays and cost increases will be incurred by the US."

The mitigation action taken was that the US took over the design of Triple electronics to be fabricated by the UK. The design phase is now over and review reports published. Production is well under way in the UK where they received an extension on the time over which their funding is available. We are in close liaison with them to ensure that delivery of items meets the revised installation schedule.

9. Conclusions

We have presented details of the final design of the HAM Large Triple Suspension (HLTS) which will be used to suspend the large optics within the recycling cavities, PR3 and SR3. As noted at the preliminary design review, there is excess residual seismic noise in both longitudinal and vertical directions at low frequencies, for longitudinal up to ~ 20 Hz and for vertical up to the 28 Hz peak. We understand that steps are being taken to see if more isolation can be provided by the HAM-ISI.

We believe our design is complete but there are three open areas which await input before we proceed to procurement for those items.

9.1 Blades

We are assessing the current round of prototype blades. When we have finished characterizing these blades and compared results from the three vendors we expect to be able to proceed with production.

9.2 Structure

We are seeking approval from the VRB for using clinch nuts in the structure. If that approval is not given we will need to redesign the structure with thicker legs.

9.3 Prisms

We need to finish assessment of the sapphire prisms, and confer with our vendor or seek an alternative vendor to ensure that our production items meet specifications.

10. Details of MATLAB model

The MATLAB set of files used to generate the sensor and seismic noise transfer functions used in figures 7 and 8 can be found in T080310-v3. We list below the key parameters and resonant frequencies used in the model. For the purposes of the MATLAB model, which assumes symmetry, the optic is modeled as a symmetric right circular cylinder of radius 132.5 mm and thickness 100 mm to give the correct mass. All units are SI. Diagrams and further information explaining the parameter nomenclature are given in sections 11.1 and 11.2.

m1: 1.1910e+001
I1x: 1.2250e-001
I1y: 1.8130e-002
I1z: 1.2370e-001
m2: 1.2150e+001
I2x: 8.2070e-002
I2y: 1.9960e-002
I2z: 8.1900e-002
tx: 1.0000e-001
tr: 1.3250e-001
m3: 1.2140e+001
I3x: 1.0656e-001
I3y: 6.3397e-002
I3z: 6.3397e-002
l1: 2.0250e-001
l2: 2.0360e-001
l3: 2.5520e-001
nw1: 2
nw2: 4
nw3: 4
r1: 3.0500e-004
r2: 1.7000e-004
r3: 1.3450e-004
Y1: 2.1200e+011

```
    Y2: 2.1200e+011
    Y3: 2.1200e+011
   l1b: 2.5000e-001
   a1b: 6.5000e-002
   h1b: 2.0500e-003
  ufc1: 2.2700e+000
   l2b: 1.2000e-001
   a2b: 3.2000e-002
   h2b: 1.1700e-003
  ufc2: 2.7300e+000
    su: 0
    si: 3.0000e-002
    sl: 5.0000e-003
    n0: 7.7000e-002
    n1: 1.3000e-001
    n2: 7.0000e-002
    n3: 1.3750e-001
    n4: 1.4050e-001
    n5: 1.4050e-001
stage2: 1
    d0: 1.0000e-003
    d1: 1.0000e-003
    d2: 1.0000e-003
    d3: 1.0000e-003
    d4: 1.0000e-003
ribbon: 0
    db: 0
     g: 9.8100e+000
   kc1: 1.2114e+003
   kc2: 1.7874e+003
   tl1: 1.9644e-001
   tl2: 1.9409e-001
   tl3: 2.5720e-001
```

l_suspoint_to_centreofoptic: 6.4773e-001

l_suspoint_to_bottomofoptic: 7.8023e-001

flex1: 2.7010e-003

flex2: 1.4001e-003

flex3: 1.3529e-003

flex3tr: 1.3529e-003

longpitch1: [6.7266e-001 7.7346e-001 1.5858e+000]

longpitch2: [2.2895e+000 2.8660e+000 3.8048e+000]

yaw: [1.0148e+000 2.2999e+000 3.3523e+000]

transroll1: [6.9292e-001 1.5234e+000 2.1505e+000]

transroll2: [2.5827e+000 4.0673e+000 4.5240e+001]

vertical: [1.1193e+000 3.8778e+000 2.8133e+001]

11. Details of Mathematica model

The Mathematica model developed by Mark Barton is described in T020205-02. A web page with further information and examples can be found under the "Triple Pendulum Model Xtra-Lite"at

http://www.ligo.caltech.edu/~e2e/SUSmodels/index.html

The relevant file used to generate the thermal noise curves in figures 7 and 8 is

```
mbtriplelite2_20100308hlts_TN;
```

Further details of the specifications set up for the modeling are given in Section 12.3, and also can be found in T1000136-v1.

In the Mathematica model the shape of the mirror with 0.6 degree vertical asymmetric wedge, thick side down, is fully included in the model (as opposed to being simplified as in the MATLAB model). The resonant frequencies (in Hz), derived from the Mathematica model, are given below. Very good agreement (generally to at least 3 significant figures) is found between these frequencies and those derived in the MATLAB model presented in section 10. The only mode which differs at the level of ~ 1% is the first pitch mode at 0.78 Hz, influenced by the vertical wedge which is fully modeled in Mathematica but not in the MATLAB code.

Stage 2:

N	f	type
1	0.6742803566926967	x3 pitch3
2	0.6927078048215571	y3

3	0.7836047716544399	pitch3	x3	
4	1.0147674610333492	yaw3	yaw2	
5	1.1192578834327849	z3	z2	
6	1.524559395433255	y2	y3	y1
7	1.5857320411266325	x2	x1	
8	2.1511552077311724	roll3	roll2	y1
9	2.2902919289717385	pitch1		
10	2.2999126183220886	yaw1	yaw3	
11	2.58288984129054	roll1	y1	
12	2.866035918714002	x1		
13	3.3524105253177097	yaw2	yaw1	
14	3.804892903771545	pitch2		
15	3.877761201309095	z1		
16	4.067326720355675	y1	roll1	roll3
17	28.13262590431044	z2	z3	
18	45.23911671958286	roll2	roll3	

12. Appendices

12.1 Diagrams Showing Triple Pendulum Parameters

The parameters for a triple pendulum (face on view).

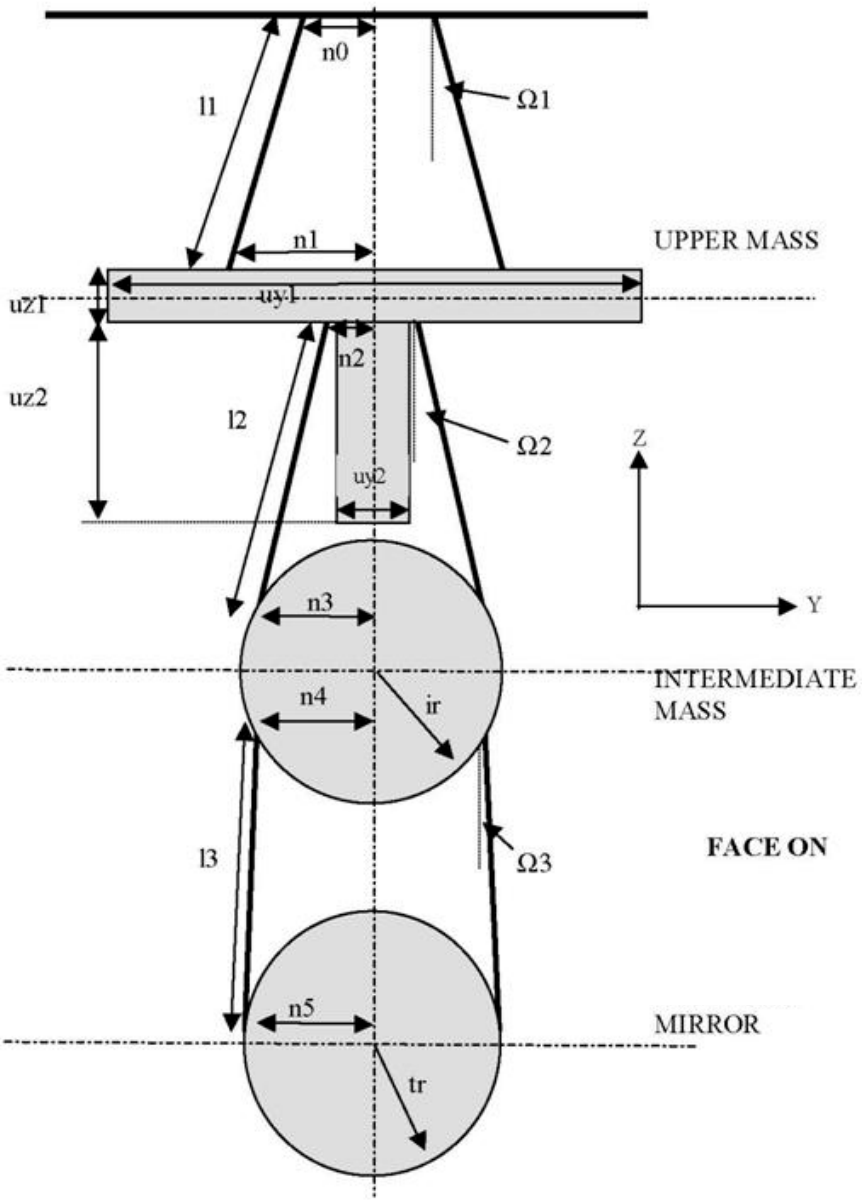

The parameters of a triple pendulum (side view).

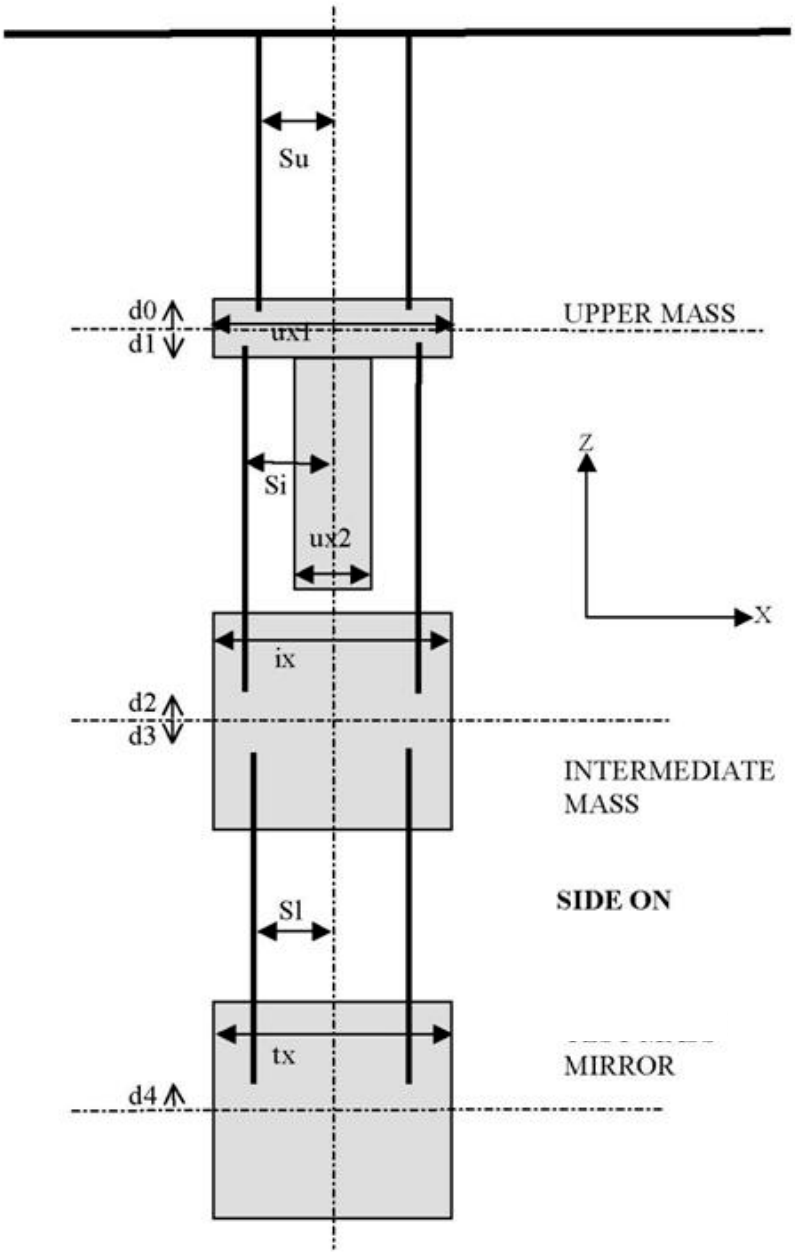

12.2 Explanation of parameters listed in section 10 (other than those shown in the diagrams above).

m1, m2, m3: masses from top to bottom

Iix, Iiy, Iiz where i = 1,2,3 from top to bottom mass = moments of inertia as follows
Iix: moment of inertia (transverse roll)
Iiy: moment of inertia (longitudinal pitch)
Iiz: moment of inertia (yaw)

nwi = number of suspension wires at each stage from top to bottom

ri = wire radius from top to bottom

Yi = Young's modulus of wire/fibre from top to bottom

l1b, a1b, h1b: length, width at root, thickness of top blades

ufc1: uncoupled frequency of top blade with mass immediately below it

l2b etc – same as above for lower blades

stage 2 = 1
If pend.stage2 is defined and non-zero, d0-d4 are interpreted as raw values, i.e., as actual wire breakoff vertical positions

tl1, tl2, tl3: centre to centre vertical separations at each stage - from top suspension point to centre of top mass, centre of top mass to centre of intermediate mass, and centre of intermediate mass to centre of beamsplitter optic respectively

ribbon = 0: round wires/fibres are used (i.e not ribbons)

db = 0: no natural damping included

g: accel. due to gravity

kc1, kc2: blade stiffness (top and bottom respectively)

l_suspoint_to_centreofoptic: length from top suspension point to centre of topic = tl1+tl2+tl3

l_suspoint_to_bottomofoptic: length from top suspension point to bottom of optic

flex1, flex2, flex3: flexure length for wire (top to bottom respectively)

flextr – flexure length for ribbon in transverse/roll direction (same as flex3 if round fibre used)

12.3 Further specifications used in the Mathematica model

Model: GEO-style triple pendulum xtra-lite

Case: 20100308hlts

Norna's HLTS parameter set of 3/8/10 plus intended 0.6 degree vertical wedge (asymmetrical, bottom-heavy, front face vertical)

overrides:

lockedblades -> False

kw1usual -> (A1*Y1)/l1

kw2usual -> (A2*Y2)/l2

kw3usual -> (A3*Y3)/l3

kbuzusual -> 19.739208802178716*m1*ufc1^2

kblzusual -> 9.869604401089358*m2*ufc2^2

kw1 -> If[lockedblades, recipadd[kw1usual, kbuzusual], kw1usual]

kw2 -> If[lockedblades, recipadd[kw2usual, kblzusual], kw2usual]

kw3 -> kw3usual

kbuz -> If[lockedblades, 10^4*kbuzusual, kbuzusual]

kblz -> If[lockedblades, 10^4*kblzusual, kblzusual]

kbuy -> If[lockedblades, 10^4*kbuzusual, 10^4*kbuzusual]

kbly -> If[lockedblades, 10^4*kblzusual, 10^4*kblzusual]

kbux -> If[lockedblades, 10^4*kbuzusual, 10^2*kbuzusual]

kblx -> If[lockedblades, 10^4*kblzusual, 10^2*kblzusual]

mbeu -> 0

mbel -> 0

den1 -> 4000

ux -> 0.1

uy -> 0.3

uz -> 0.06

I1x -> 0.1225

I1y -> 0.01813

I1z -> 0.1237

m1 -> 11.91

den2 -> 2202

ix -> 0.1

ir -> 0.255

m2 -> 12.15

I2x -> 0.08207

I2y -> 0.01996

I2z -> 0.0819

COM2y -> -COM3y

I2xy -> -I3xy

wedge -> 0.010471975511965978

tx -> 0.1014 - tr*wedge

tr -> 0.1325

den3 -> 2201

wabh3 -> 0

wabv3 -> wedge

wafh3 -> 0

wafv3 -> 0

m3 -> 3.141592653589793*den3*tr^2*tx

I3x -> (den3*Pi*tr^4*tx)/2

I3y -> (den3*Pi*tr^2*tx*(2*tx^2 + 3*tr^2*(2 + wabh3^2 + wabv3^2 + wafh3^2 + wafv3^2)))/24

I3z -> (den3*Pi*tr^2*tx*(2*tx^2 + 3*tr^2*(2 + wabh3^2 + wabv3^2 + wafh3^2 + wafv3^2)))/24

I3zx -> (den3*Pi*tr^4*tx*(wabv3 + wafv3))/8

I3xy -> (den3*Pi*tr^4*tx*(wabh3 + wafh3))/8

I3yz -> 0

COM3x -> -(tr^2*(wabh3^2 + wabv3^2 - wafh3^2 + wafv3^2))/(8*tx)

COM3y -> (tr^2*(-wabh3 + wafh3))/(4*tx)

COM3z -> (tr^2*(-wabv3 + wafv3))/(4*tx)

FRP3x -> COM3x

l1 -> 0.2025

l2 -> 0.2036

l3 -> 0.2552

r1 -> 0.000305

r2 -> 0.00016999999999999999

r3 -> 0.0001345

bssteel -> 2000000000

wssilica -> 7.7*^8

r1opt -> 0.9772050238058398*Sqrt[(g*(m1 + m2 + m3))/(bssteel*c1*nw1)]

r2opt -> 0.9772050238058398*Sqrt[(g*(m2 + m3))/(bssteel*c2*nw2)]

r3opt -> 0.5641895835477563*Sqrt[(g*m3)/(c3*nw3*wssilica)]

Y1 -> Ysteel

Y2 -> Ysteel

Y3 -> Ysteel

ufc1 -> 2.27

ufc2 -> 2.73

d0 -> 0.001

d1 -> 0.001

d2 -> 0.001

d3 -> 0.001

d4 -> 0.001

dl -> 0

su -> 0

si -> 0.03

sl -> 0.005

n0 -> 0.077

n1 -> 0.13

n2 -> 0.07

n3 -> 0.1375

n4 -> 0.1405

n5 -> 0.1405

flex1 -> c1^(3/2)*Sqrt[(M11*nw1*Y1)/(g*(m1 + m2 + m3))]

flex2 -> c2^(3/2)*Sqrt[(M21*nw2*Y2)/(g*(m2 + m3))]

flex3 -> c3^(3/2)*Sqrt[(M31*nw3*Y3)/(g*m3)]

rhosilica -> 2200.

Csilica -> 772.

Ksilica -> 1.38

alphasilica -> 3.8999999999999997*^-7

betasilica -> 0.000152

Ysilica -> 7.2*^10

phisilica -> 4.1*^-10

phissilica -> 3.*^-11

dssilica -> 0.015

rhosteel -> 7800.

Csteel -> 486.

Ksteel -> 49.

alphasteel -> 0.000012

betasteel -> -0.00025

phisteel -> 0.0002

Ysteel -> 2.12*^11

rhomarag -> 7800.

Cmarag -> 460.

Kmarag -> 20.

alphamarag -> 0.000011

betamarag -> -0.00025

phimarag -> 0.0001

Ymarag -> 1.87*^11

magicnumber -> 0.07374723253051044

tmU -> 0.0025

tmL -> 0.0017

deltabladeU -> (alphamarag^2*temperature*Ymarag)/(Cmarag*rhomarag)

deltabladeL -> (alphamarag^2*temperature*Ymarag)/(Cmarag*rhomarag)

deltawireU -> (temperature*(alphasteel - (0.3183098861837907*betasteel*g*(m1 + m2 + m3))/(nw1*r1^2*Ysteel))^2*Ysteel)/(Csteel*rhosteel)

deltawireL -> (temperature*(alphasteel - (0.3183098861837907*betasteel*g*(m2 + m3))/(nw2*r2^2*Ysteel))^2*Ysteel)/(Csteel*rhosteel)

deltafibre -> (temperature*(alphasteel - (0.3183098861837907*betasteel*g*m3)/(nw3*r3^2*Ysteel))^2*Ysteel)/(Csteel*rhosteel)

taubladeU -> (0.10132118364233778*Cmarag*rhomarag*tmU^2)/Kmarag

taubladeL -> (0.10132118364233778*Cmarag*rhomarag*tmL^2)/Kmarag

tauwireU -> (4*Csteel*magicnumber*r1^2*rhosteel)/Ksteel

tauwireL -> (4*Csteel*magicnumber*r2^2*rhosteel)/Ksteel

taufibre -> (4*Csteel*magicnumber*r3^2*rhosteel)/Ksteel

damping[imag, bladeUtype] -> (phimarag + (deltabladeU*(2*N[Pi]*#1*taubladeU))/(1 + (2*N[Pi]*#1*taubladeU)^2) &)

damping[imag, bladeLtype] -> (phimarag + (deltabladeL*(2*N[Pi]*#1*taubladeL))/(1 + (2*N[Pi]*#1*taubladeL)^2) &)

damping[imag, wireUtype] -> (phisteel &)

damping[imag, wireLtype] -> (phisteel &)

damping[imag, wireUatype] -> (phisteel + (deltawireU*(2*N[Pi]*#1*tauwireU))/(1 + (2*N[Pi]*#1*tauwireU)^2) &)

damping[imag, wireLatype] -> (phisteel + (deltawireL*(2*N[Pi]*#1*tauwireL))/(1 + (2*N[Pi]*#1*tauwireL)^2) &)

damping[imag, fibretype] -> (phisteel &)

damping[imag, fibreatype] -> (phisteel + (deltafibre*(2*N[Pi]*#1*taufibre))/(1 + (2*N[Pi]*#1*taufibre)^2) &)

constval:

g -> 9.81

ux -> 0.1

uy -> 0.3

uz -> 0.06

den1 -> 4000

m1 -> 11.91

I1x -> 0.1225

I1y -> 0.01813

I1z -> 0.1237

ix -> 0.1

ir -> 0.255

den2 -> 2202

m2 -> 12.15

I2x -> 0.08207

I2y -> 0.01996

I2z -> 0.0819

tx -> 0.1000124632446645

tr -> 0.1325

den3 -> 2201

m3 -> 12.141037362636423

I3x -> 0.10657554359889287

I3y -> 0.06341074686649308

I3z -> 0.06341074686649308

l1 -> 0.2025

l2 -> 0.2036

l3 -> 0.2552

nw1 -> 2

nw2 -> 4

nw3 -> 4

r1 -> 0.000305

r2 -> 0.00016999999999999999

r3 -> 0.0001345

Y1 -> 2.12*^11

Y2 -> 2.12*^11

Y3 -> 2.12*^11

ufc1 -> 2.27

ufc2 -> 2.73

ufc3 -> 0

d0 -> 0.001

d1 -> 0.001

d2 -> 0.001

d3 -> 0.001

d4 -> 0.001

su -> 0

si -> 0.03

sl -> 0.005

n0 -> 0.077

n1 -> 0.13

n2 -> 0.07

n3 -> 0.1375

n4 -> 0.1405

n5 -> 0.1405

tl1 -> 0.19644116761828867

tl2 -> 0.1940851634041526

tl3 -> 0.2572

ltotal -> 0.6477263310224413

leverarmrt -> 0.03

leverarmrz -> 0.08

leverarmrl -> 0.08

gain -> 0.4

gainrtzrtl -> 0.4

gaint -> 0.8

gainlrz -> 0.4

b1 -> 0.03

b2 -> 0.03

b3 -> 0.03

b4 -> 0.03

b5 -> 0.03

b6 -> 0.03

unstretched -> False

vertblades -> True

ul1 -> 0.20189867588383673

ul2 -> 0.2029320664974043

ul3 -> 0.254569311111847

sl1 -> 0.2025

sl2 -> 0.2036

sl3 -> 0.2552

si1 -> 0.2617283950617284

si2 -> 0.33153241650294696

si3 -> 0.

c1 -> 0.9651415684853761

c2 -> 0.9434438281146984

c3 -> 1.

pitchbul -> 0

pitchbur -> 0

pitchbll -> 0

pitchblr -> 0

pitchbllf -> 0

pitchblrf -> 0

pitchbllb -> 0

pitchblrb -> 0

rollbul -> 0

rollbur -> 0

rollbll -> 0

rollblr -> 0

rollbllf -> 0

rollblrf -> 0

rollbllb -> 0

rollblrb -> 0

A1 -> 2.922466566001905*^-7

A2 -> 9.0792027688745*^-8

A3 -> 5.683219650160275*^-8

kw1 -> 305956.9935764957

kw2 -> 94537.86773091326

kw3 -> 47211.6992881653

kbuz -> 1211.4157532276533

kblz -> 893.7196718866784

bdu -> 0.1465773313502246

bdl -> 0.06665822741274476

I1xy -> 0

I1yz -> 0

I1zx -> 0

COM1x -> 0

COM1y -> 0

COM1z -> 0

FRP1x -> 0

FRP1y -> 0

FRP1z -> 0

Ibtxyl -> 0

Ibtyzl -> 0

Ibtzxl -> 0

I2xy -> 0

I2yz -> 0

I2zx -> 0

COM2x -> 0

COM2y -> 0

COM2z -> 0

FRP2x -> 0

FRP2y -> 0

FRP2z -> 0

I3xy -> 0

I3yz -> 0

I3zx -> 0.00027901412068551714

COM3x -> -2.406272909578665*^-6

COM3y -> 0

COM3z -> -0.0004595642735850743

FRP3x -> -2.406272909578665*^-6

FRP3y -> 0

FRP3z -> 0

btx -> 0.03

bty -> 0.03

btz -> 0.03

phib -> 0.001

M11 -> 6.796561307558179*^-15

M12 -> 6.796561307558179*^-15

M21 -> 6.559724000511825*^-16

M22 -> 6.559724000511825*^-16

M31 -> 2.570271606907798*^-16

M32 -> 2.570271606907798*^-16

temperature -> 290.
boltzmann -> 1.380658*^-23
alphasilica -> 3.8999999999999997*^-7
betasilica -> 0.000152
rhosilica -> 2200.
Csilica -> 772.
Ksilica -> 1.38
Ysilica -> 7.2*^10
phisilica -> 4.1*^-10
phissilica -> 3.*^-11
rhosteel -> 7800.
Csteel -> 486.
Ksteel -> 49.
Ysteel -> 2.12*^11
alphasteel -> 0.000012
betasteel -> -0.00025
phisteel -> 0.0002
rhomarag -> 7800.
Cmarag -> 460.
Kmarag -> 20.
Ymarag -> 1.87*^11
alphamarag -> 0.000011
betamarag -> -0.00025
phimarag -> 0.0001
tmU -> 0.0025
tmL -> 0.0017
magicnumber -> 0.07374723253051044
deltabladeU -> 0.0018288266443701228
deltabladeL -> 0.0018288266443701228
deltawireU -> 0.0026226358956784154
deltawireL -> 0.0026463124831431215
deltafibre -> 0.002582098894278859
taubladeU -> 0.11360637715897123

taubladeL -> 0.0525315887983083

tauwireU -> 0.0021229520709678527

tauwireL -> 0.0006595357683522809

tausilica -> 0.009063381660749428

damping[imag, bladeUtype] -> (0.0001 + (0.0013054346002858645*#1)/(1 + 0.509524601557986*#1^2) &)

damping[imag, bladeLtype] -> (0.0001 + (0.0006036329591721838*#1)/(1 + 0.10894337087161483*#1^2) &)

damping[imag, wireUtype] -> (0.0002 &)

damping[imag, wireLtype] -> (0.0002 &)

damping[imag, wireUatype] -> (0.0002 + (0.0000349830812537838 66*#1)/(1 + 0.00017792628682807625*#1^2) &)

damping[imag, wireLatype] -> (0.0002 + (0.0000109662804243678 49*#1)/(1 + 0.00001717261540376522*#1^2) &)

damping[imag, fibretype] -> (0.0002 &)

damping[imag, fibreatype] -> (0.0002 + (6.697887048570391*^-6*#1)/(1 + 6.728680320269774*^-6*#1^2) &)

x00 -> 0

y00 -> 0

z00 -> 0

yaw00 -> 0

pitch00 -> 0

roll00 -> 0

kconx1 -> 0

kcony1 -> 0

kconz1 -> 0

kconyaw1 -> 0

kconpitch1 -> 0

kconroll1 -> 0

kconx2 -> 0

kcony2 -> 0

kconz2 -> 0

kconyaw2 -> 0

kconpitch2 -> 0

kconroll2 -> 0

kconx3 -> 0

kcony3 -> 0

kconz3 -> 0

kconyaw3 -> 0

kconpitch3 -> 0

kconroll3 -> 0

lockedblades -> False

kw1usual -> 305956.9935764957

kw2usual -> 94537.86773091326

kw3usual -> 47211.6992881653

kbuzusual -> 1211.4157532276533

kblzusual -> 893.7196718866784

kbuy -> 1.2114157532276532*^7

kbly -> 8.937196718866784*^6

kbux -> 121141.57532276532

kblx -> 89371.96718866783

mbeu -> 0

mbel -> 0

wedge -> 0.010471975511965978

wabh3 -> 0

wabv3 -> 0.010471975511965978

wafh3 -> 0

wafv3 -> 0

bssteel -> 2000000000

wssilica -> 7.7*^8

r1opt -> 0.0002963843012298175

r2opt -> 0.00017363617422581746

r3opt -> 0.00011094611697983105

dl -> 0

flex1 -> 0.0027009656914013277

flex2 -> 0.0014000941676377084

flex3 -> 0.0013527733345524236

dssilica -> 0.015

taufibre -> 0.000412843146485635

optval:

{x1, 0.}

{y1, 0.}

{z1, -0.19644116761828867}

{yaw1, 0.}

{pitch1, 0.}

{roll1, 0.}

{x2, 0.}

{y2, 0.}

{z2, -0.3905263310224413}

{yaw2, 0.}

{pitch2, 0.}

{roll2, 0.}

{x3, 2.406272909578665*^-6}

{y3, 0.}

{z3, -0.6477263310224413}

{yaw3, 0.}

{pitch3, 0.}

{roll3, 0.}

{qul, 0.}

{qur, 0.}

{qlf, 0.}

{qlb, 0.}

{qrf, 0.}

{qrb, 0.}

12.4 Seismic input for noise curves

seisHAM.m (supplied by Peter F)

```
% [ampX, ampZ, ampRX, ampRZ, ampSP] = seisHAM(f)
%   displacement amplitude spectrum of HAM ISI table
%
% based on data from
% http://ilog.ligo-
wa.caltech.edu/ilog/pub/ilog.cgi?group=detector&date_to_view=
% 07/17/2008&anchor_to_scroll_to=2008:07:18:07:34:50-blantz
% and the proposed HAM HEPI X-beam modification (see HAM ISI PDR)
%
% note that ampY and ampRY are assumed to be equal to ampX and ampRX
% ampSP is the suspension point motion for the targeted HAM ISI requirement

function [ampX, ampZ, ampRX, ampRZ, ampSP] = seisHAM(f)

  % frequency, ampX, ampZ, ampRX, ampRZ
  fa = [1e-3 1e-6 1e-6 1e-7 1e-7
    0.1 1e-6 4e-7 4e-8 3e-7
    0.2 5e-7 3e-7 2e-8 4e-8
    0.3 1e-7 1e-7 5e-9 1e-8
    0.4 3e-8 3e-8 3e-9 4e-9
    0.5 1e-8 1e-8 1e-9 2e-9
    0.6 2e-9 2e-9 8e-10 8e-10
    0.7 4e-10 2e-10 8e-11 1e-10
    0.8 5e-10 3e-10 1e-10 2e-10
    1.0 3e-10 4e-10 8e-11 1.5e-10
    1.4 6e-11 1e-10 1.5e-11 4e-11
    2 2e-11 3e-11 1e-11 3e-11
    5 2.2e-11 4e-11 7e-12 2e-11
    10 3e-11 6e-11 3e-12 4e-12
    13 4e-11 8e-11 4e-12 2e-12
    15 5e-11 1e-10 6e-12 1.5e-12
    18 4e-11 6e-11 4e-12 1e-12
    24 7e-12 8e-12 1.5e-12 6e-13
    30 3e-12 3e-12 1e-12 3e-13
    60 3e-13 3e-13 1.5e-13 8e-14
    100 6e-14 6e-14 3e-14 2e-14
    1e3 1e-14 1e-14 1e-14 1e-14
    1e4 1e-15 1e-15 1e-15 1e-15];

  ampX = exp(interp1(log(fa(:,1)), log(fa(:,2)), log(f), 'cubic'));
  ampZ = exp(interp1(log(fa(:,1)), log(fa(:,3)), log(f), 'cubic'));
  ampRX = exp(interp1(log(fa(:,1)), log(fa(:,4)), log(f), 'cubic'));
  ampRZ = exp(interp1(log(fa(:,1)), log(fa(:,5)), log(f), 'cubic'));

  % proposed requirement displacement noise
  % frequency, ampSP (Suspension Point)

  faSP = [1e-2 4e-6
      0.1 4e-7
```

```
      0.2 2e-7
      0.6 6.66e-10
      1.0 4.0e-10
      10 4.0e-11
      30 1.33e-11
      100 1.33e-11];

  ampSP = exp(interp1(log(faSP(:,1)), log(faSP(:,2)), log(f), 'cubic'));
```

12.5 Control Law used for Damping

GEO active filter design as used in MATLAB model:

Consists of a lowpass, a high pass and two transitional differentiators as follows

lowpass(fcut,dcGain) with values (9, 1)

highpass(fcut,hfGain) with values (0.7,1)

transdif(lf,hf,dcGain) with values (0.35,0.7,1) and (1,9,1)

where the functions are

lowpass
z = [];
p = -2*pi*fcut;
k = dcGain*2*pi*fcut;

highpass
z = 0;
p = -2*pi*fcut;
k = hfGain;

transdif
z = -2*pi*lf;
p = -2*pi*hf;
k = dcGain*(hf/lf);

Bode diagram shown below.

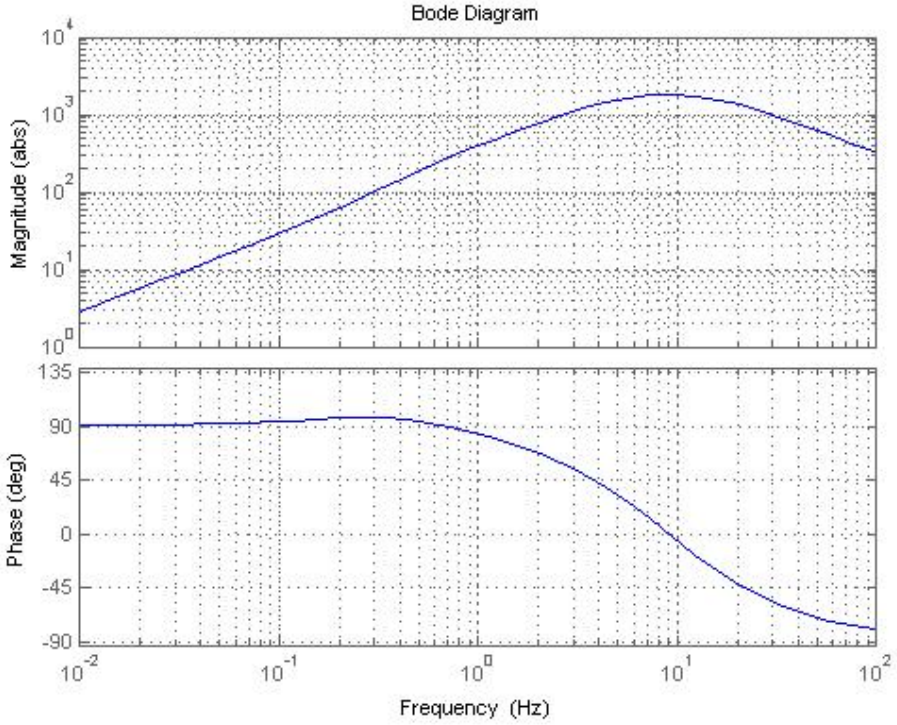
Bode Diagram
Magnitude (abs)
Phase (deg)
Frequency (Hz)